Technical Paper

大 韓 造 船 學 會 誌
第27卷 第4號 1990年 12月
Journal of the Society of
Naval Architects of Korea
Vol. 25, No. 4, December 1960

Numerical Calculation of the Flow around a Ship by Means of Rankine Source Distribution

by

Jae-Shin Kim*, Kwi-Joo Lee* and Soon-Won Joa*

Rankine Source 분포를 이용한 선체주위 자유표면류의 수치계산

김 재 신*, 이 귀 주*, 좌 순 원*

Abstract

The method using Rankine Soure distribution over the hull surface and undisturbed free surface was applied to calculate the free surface flow around a ship. The ship hull as well as a local portion of the undisturbed free surface are geometrically represented by quadrilateral panels and the source density is determined so as to satisfy the linearized free surface condition based on the double model flow.

The pressure distribution, wave resistance, wave profile and hydrodynamic sinkage force and trim moment for the Wigley hull and the Series 60 hull with C_B=0.60 were calculated in the fixed condition. The calculated results were compared with the measured values. The dependance of the solution on the panel arrangement, particularly on the free suraface, was also studied through 11 numerical test cases for the Wigley hull.

요 약

선체표면 및 자유표면에 Rankine Source를 분포하는 방법에 의하여 선체 주위의 유동의 수치계산을 수행하였다. 선체표면 및 자유표면은 사각형 Panel들로 표시되며 자유표면 조건은 이중모형흐름에 의해 선형화 되어 C.W. Dawson의 유한 차분법에 따라 교란없는 자유표면에 적용되었다.

Wigley 선형 및 Series 60, C_B=0.6 선형에 대한 Fixed Condition에서의 조파저항, 선측파고, 압력분포 및 Trim & Sinkage 등을 계산하였으며 계산된 결과는 국내외 수조에서의 계측치와 비교하였다. 또한, 선체표면과 자유표면의 Panel 분할조건 및 자유표면의 선경영역의 변화에 따른 계산치의 영향도 아울러 조사하였다.

1. Introduction

Since the surface source method to calculate the potential flow about arbitrary three-dimensional bodies has been developed by Hess & Smith [1], the Rankine source panel method taking the free surface effect into account is studied to deal with the problems of ship wave and wave resistance by Gadd, Dawson, Mori, Ogiwara, etc.[2, 3, 4, 5]. Then

발표 : 1989년도 대한조선학회 추계연구발표회 (1989.11.11)
Manuscript received: December 2, 1989, revised manuscript received: August 28, 1990
* Member, Hyundai Maritime Research Institute

remarkable improvements have been made so that this method is now accepted as a useful evaluation tool of practcal ship design[6, 7, 8].

The computer program (WRES1) of HMRI based on the Rankine source method was tentatively applied to calculate the free surface flow around the Wigley hull and the Series 60 hull, $C_B=0.60$.

The ship hull as well as a local portion of the undisturbed free surface are geometrically represented by quadrilateral panels and the source density is determined so as to satisfy the linearized free surface condition based on the double model flow.

The local flow field, pressure distribution, wave resistance, wave profile and hydrodynamic sinkage force and trim moment for two ships were calculated in the fixed condition and the results were compared with the measured values. Through numerical test cases with the different panel arrangement on the hull surface and particularly on the free surface, the dependence of the numerical solution on the panel arrangement was also studied.

2. Fundamental Formulation

The coordinate system $O\text{-}xyz$ is fixed to the hull with its origin on the midship section, the $x-y$ plane coincides with the undisturbed free surface, the x-axis is in the direction of uniform flow, and the z-axis vertically upward.

The velocity potential ϕ must satisfy the following conditions:

$$\nabla^2\phi=0 \qquad (1)$$

$$\phi_n=0 \qquad \text{on ship hull So} \qquad (2)$$

$$g\zeta+1/2(\phi_x^2+\phi_y^2+\phi_z^2-U^2)=0 \quad \text{at } z=\zeta(x,y) \qquad (3)$$

$$\phi_x\zeta_x+\phi_y\zeta_y-\phi_z=0 \qquad \text{at } z=\zeta(x,y) \qquad (4)$$

Eliminating ζ from eqs. (3) and (4),

$$1/2[\phi_x(\nabla\phi\cdot\nabla\phi)_x+\phi_y(\nabla\phi\cdot\nabla\phi)_y +\phi_z(\nabla\phi\cdot\nabla\phi)_z]+g\phi_z=0 \qquad \text{at } z=\zeta(x,y) \qquad (5)$$

The total velocity potential is expressed by the sum of a double model velocity potential Φ and a potential ψ representing the effect of free wave,

$$\phi=\Phi+\psi \qquad (6)$$

Substituting eq. (6) into eq. (5) eq., (5) can be linearized about the double model velocity potential Φ by neglecting the non-linear terms of ψ and assuming that eq. (5) holds on $z=0$ instead of on the free surface, that is

$$2\Phi_l\Phi_{ll}\phi_l+\Phi_l^2\phi_{ll}+g\phi_z=2\Phi_l^2\Phi_{ll} \qquad (7)$$

where the subscript l denotes differentiation along a stream line of the double model potential Φ on the symmetry plane $z=0$.

Replacing ψ with $\phi-\Phi$ in eq.(7), We get Dawson's double-hull-linearized free surface condition as follows[3, 4].

$$(\Phi_l^2\phi_l)_l+g\phi_z=2\Phi_l^2\Phi_{ll} \qquad (8)$$

Φ_{ll} is expressed by the upstream, finite difference method and such method satisfies the radiation condition[9]. And it has been also proved by C.S. Lee, et al [10] that the Rankine Sources distributedon the still water surface generate the radiation waves.

3. Method of Numerical Calculation

The total velocity potential ϕ may be represented as

$$\phi(x,y,z)=Ux+\iint_s \frac{\sigma(q)}{r(p,q)}ds \qquad (9)$$

where σ is the source density, r is the distance from the integration point $q(x',y',z')$ on S to the field point $p(x,y,z)$ where the potential is being evaluated. The integration domain S consists of the surface and the undisturbed local free surface.

The numerical procedure begins with the discretization of the integration domain S so that integration is replaced by summation. Both the hull surface and the undisturbed local free surface are divided into quadrilateral panels. Each panel is characterized by its null point, normal vector and various geometrical properties such as surface area and second moment. The source density over each panel is supposed to be constant. The velocity components at the null point of the i-th panel may be obtained from

$$\phi_{xi}=U+\sum_{j=1}^{M_t}\sigma_jX_{ij}$$

$$\phi_{yi}=\sum_{j=1}^{M_t}\sigma_jY_{ij} \qquad (10)$$

$$\phi_{zi}=\sum_{j=1}^{M_1}\sigma_j Z_{ij}$$

where M_1 is the number of panels, X_{ij}, Y_{ij} and Z_{ij} are the velocity components induced at the null point of the i-th panel by a unit source density on the j-th panel.

On the hull surface, the boundary condition of eq. (2) must be satisfied at the null point of each panel [11].

$$\sum_{j=1}^{M_1}(X_{ij}N_{xi}+Y_{ij}N_{yi}+Z_{ij}N_{zi})\sigma_j=-UN_{xi} \quad (11)$$

where (N_{xi}, N_{yi}, N_{zi}) is the unit normal vector to the i-th panel.

For the panels on the free surface the normal direction is replaced by the l direction. The l direction vector at each null point is determined as

$$L_{xi}=\frac{\Phi_{xi}}{(\Phi^2_{xi}+\Phi^2_{yi})^{1/2}} \quad (12)$$

$$L_{yi}=\frac{\Phi_{yi}}{(\Phi^2_{xi}+\Phi^2_{yi})^{1/2}}$$

$$L_{zi}=0$$

where

$$\Phi_{xi}=U+\sum_{j=1}^{M}\sigma_{0j}X_{ij} \quad (13)$$

$$\Phi_{yi}=\sum_{j=1}^{M}\sigma_{0j}Y_{ij}$$

and σ_{0j} are obtained from the double-model solution. At the free surface σ_{0j} has a value of zero.

For each panel on the free surface, the terms in eq. (8) may be expressed as

$$\phi_{li}=\phi_{xi}L_{xi}+\phi_{yi}L_{yi}$$

$$=UL_{xi}+\sum_{j=1}^{M}(X_{ij}L_{xi}+Y_{ij}L_{yi})\sigma_j \quad (14)$$

$$(\Phi_l^2\phi_l)_i=\Phi_{li}^2 UL_{xi}+\Phi_{li}^2*\sum_{j=1}^{M}(X_{ij}L_{xi}+Y_{ij}L_{yi})\sigma_j \quad (15)$$

The finite difference operator used by Dawson [3] is used to obtain Φ_{ll} and $(\Phi^2\phi_l)_l$

$$\Phi_{lli}=CA_i\Phi_{li}+CB_i\Phi_{li-1}+CC_i\Phi_{li-2}+CD_i\Phi_{li-3} \quad (16)$$

$$(\Phi_l^2\phi_l)_{li}=CA_i\Phi^2_{li}UL_{xi}+CB_i\Phi^2_{li-1}UL_{xi-1}$$

$$+CC_i\Phi^2_{li-2}UL_{xi-2}+CD_i\Phi^2_{li-3}UL_{xi-3}$$

$$+\sum_{j=1}^{M}[CA_i\Phi^2_{li}(X_{ij}L_{xi}+Y_{ij}L_{yi})$$

$$+CB_i\Phi^2_{li-1}(X_{i-1j}L_{xi-1}+Y_{i-1j}L_{yi-1})$$

$$+CC_i\Phi^2_{li-2}(X_{i-2j}L_{xi-2}+Y_{i-2j}L_{yi-2})$$

$$+CD_i\Phi^2_{li-3}(X_{i-3j}L_{xi-3}+Y_{i-3j}L_{yi-3}]\sigma_j \quad (17)$$

where CA_i, CB_i, CC_i and CD_i, the coefficients of the four point operator, are approximately calculated from

$$CD_i=l_1^2\cdot l_2\cdot(l_1+l_2)^2\cdot(2l_1+l_2)/D_i$$

$$CC_i=-l_1^2\cdot(l_1+l_2+l_3)^2\cdot(l_2+l_3)\cdot(2l_1+l_2+l_3)/D_i$$

$$CB_i=l_3\cdot(l_1+l_2)^2\cdot(l_1+l_2+l_2)^2\cdot(2l_1+2l_2+l_3)/D_i$$

$$CA_i=-(CB_i+CC_i+CD_i) \quad (18)$$

and

$$D_i=l_1\cdot l_2\cdot l_3\cdot(l_1+l_2)\cdot(l_2+l_3)\cdot(l_1+l_2+l_3)\cdot(3l_1+2l_2+l_3)$$

$$l_1=-[(x_{ni}-x_{ni-1})^2+(y_{ni}-y_{ni-1})^2]^{1/2}$$

$$l_2=-[(x_{ni-1}-x_{ni-2})^2+(y_{ni-1}-y_{ni-2})^2]^{1/2}$$

$$l_3=-[(x_{ni-2}-x_{ni-3})^2+(_{ni-2}-y_{ni-3})^2]^{1/2} \quad (19)$$

where (x_{ni}, y_{ni}), (x_{ni-1}, y_{ni-1}), (x_{ni-2}, y_{ni-2}), (x_{ni-3}, y_{ni-3}) are the null point coordinates of the i-th, $(i-1)$-th, $(i$-2)-th and (i-3)-th panels in a same longitudinal set, and i increases in the downstream direction.

Thus the boundary condition, eq. (8), at the i-th null point on the free surface is,

$$\sum_{j=1}^{M}[CA_i\Phi^2_{li}(X_{ij}L_{xi}+Y_{ij}L_{yi})+CB_i\Phi^2_{li-1}(X_{i-1j}L_{xi-1}+Y_{i-1j}L_{yi-1})$$

$$+CC_i\Phi^2_{li-2}(X_{i-2j}L_{xi-2}+Y_{i-2j}L_{yi-2})+CD_i\Phi^2_{li-3}(X_{i-3j}L_{xi-3}+Y_{i-3j}L_{yi-3})\sigma_j-2\pi\sigma_i$$

$$=2\Phi^2_{li}(CA_i\Phi^2_{li}+CB_i\Phi_{li-1}+CC_i\Phi_{li-2}CD_i\Phi_{li-3})$$

$$-(CA_i\Phi^2_{li}UL_{xi}+CB_i\Phi^2_{li-1}UL_{xi-1}+CC_i\Phi^2_{li-2}UL_{xi-2}+CD_i\Phi^2_{li-3}UL_{xi-3}) \quad (20)$$

The complete sets of eq. (11) and (20) compose a system of M equations in M unknown values of σ that is solved by Gaussian Elimination. With the values of the source density on all panels, the full velocities can be calculated.

Then the pressure coefficient is

$$C_{pi}=1-(V_{xi}^2+V_{yi}^2+V_{zi}^2)/U^2$$

An integration of the pressure on the hull surface gives the wave resistance coefficient.

$$C_w=\frac{\sum_{i=1}^{M_1} C_{pi}N_{xi}\,\Delta S_i}{\sum_{i=1}^{M_1}\Delta S_i} \tag{21}$$

The wave elevation may be given by

$$\zeta=1/2g(U^2+\Phi_l^2-2\Phi_l\phi_l)$$

And the hydrodynamic sinkage force and trim moment are obtained as follows

$$C_z=\frac{\sum_{i=1}^{M_1} C_{pi}N_{zi}\Delta S_i}{\sum_{i=1}^{M_1}\Delta S_i} \tag{22}$$

$$C_m=\frac{\sum_{i=1}^{M_1} C_{pi}(N_{xi}z_{ni}-N_{xi}x_{ni})\Delta S_i}{\sum_{i=1}^{M_1}\Delta V_i} \tag{23}$$

where x_{ni} and z_{ni} are the coordinates of each null point and

$$\Delta V_i=\Delta S_i\cdot z_{ni}\cdot N_{zi}$$

4. Calculation Results and Discussion

4.1. Wigley Hull

The Wigley hull to be calculated is a mathematical hull with parabolic waterlines and sections, which is expressed as the following equation.

$$y=\frac{B}{2}\left[1-\left(\frac{2x}{L}\right)^2\right]\left[1-\left(\frac{z}{H}\right)^2\right]$$

Where $-L/2\leq L/2,\ -H\leq z\leq 0$

$B/L=0.10,\quad H/L=0.0625$

To see the dependence of the solution on the panel arrangement for the hull surface, especially for the free surface, a systematic variation was carried out. 11 numerical test cases were chosen as shown in Table 1, in which the number of panels on the hull and on the free surface and the extent of the free surface in x-and y-directions are given.

For example, in the run No. 2, 8 rows of panels from the keel to the undisturbed free surface and 24 divisions from FP to AP represent the hull form and the local region of the free surface extended about 5/7 of the half length of ship to the side and was represented by 8 rows of panels as shown in Fig. 1.

The wave resistance coefficients for 11 test cases were calculated and were compared with the measurement results, reported by the Resistance Committee of the 17th ITTC [12], as shown in Fig. 2.

In numerical runs of the run No. 1, 2 and 3, the panel arrangement for the hull was changed respectively. The calculated values of No. 2, 3 with the variation of number of divisions in z-direction is not so different, but in runs of No. 1, 2 with the different panel arrangement in x-direction, the calculated resistances show bigger differences than the case of the run No. 2, 3.

In runs of run No. 4, 5 and 6, the free surface extent in the x-direction was changed respectively. In run No. 4, the free surface region in the x-direction was divided into 36 strips different from 40 strips of run No. 1 and in run No. 5, the free surface region before the ship was reduced. The wave resistance do not changed so much over all speed range except the value in 0.313 of Froude

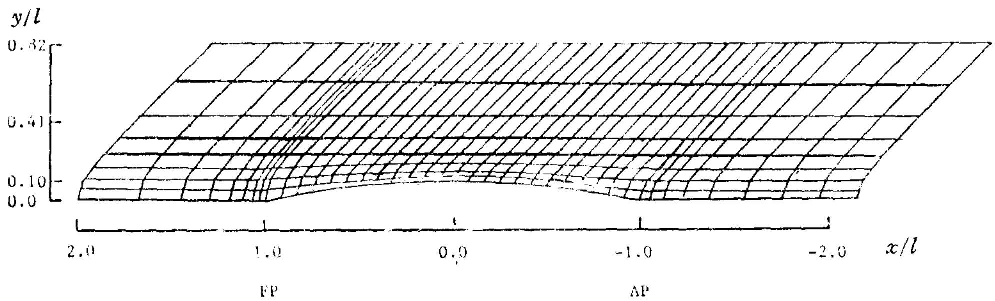

Fig. 1 Panel arrangement on the free surface for Wigley hull

Table 1 Test runs for Wigley hull (Fixed Cond.)

Run No.	Panel Arrangement (Half Range)		Extent of the Free surface (in Half Ship Length)		*Fn*	*Cw*∗10^3
	Hull	Free Surface	*x*-direction	*y*-dir.		
1	24×8	40×8	2.0∼−2.15	0.72	0.266 0.313 0.402	0.725 1.784 2.053
2	22×8	38×8	〃	〃	0.266 0.313 0.402	0.879 1.761 1.915
3	22×6	〃	〃	〃	0.266 0.313 0.402	0.873 1.754 2.103
4	24×8	36×8	2.0∼−1.5	〃	0.266 0.313 0.402	0.719 1.748 2.154
5	〃	〃	1.5∼−2.0	〃	0.266 0.313 0.402	0.742 1.680 2.100
6	〃	〃	1.5∼−1.5	〃	0.266 0.313 0.402	0.766 1.764 2.177
7	22×6	38×6	2.0∼−2.15	0.72	0.266 0.313 0.402	0.821 1.743 2.043
8	〃	38×8	〃	0.775	0.266 0.313 0.402	0.953 1.750 2.193
9	〃	〃	2.0∼−2.0	0.775	0.266 0.313 0.402	0.945 1.740 2.210
10	〃	38×10	2.0∼−2.0	0.775	0.266 0.313 0.402	0.900 1.694 1.976
11	22×8	34×8	1.75∼−1.75	0.75	0.266 0.313 0.402	0.690 1.726 2.014

No. of run No.5, which is a questionable point. In the run No. 7, 8 and 9, the free surface region in the *y*-direction was divided into 6 strips different from 8 strips of run No.2 and was enlarged by about 7/9 of the half ship length. The calculated results for run No.2, 7, 8 and 9 show the bigger difference than those for the variations of *x*-direction.

The wave resistance of run No.8 is increased by about 16% at the value of Froude No. being 0.266

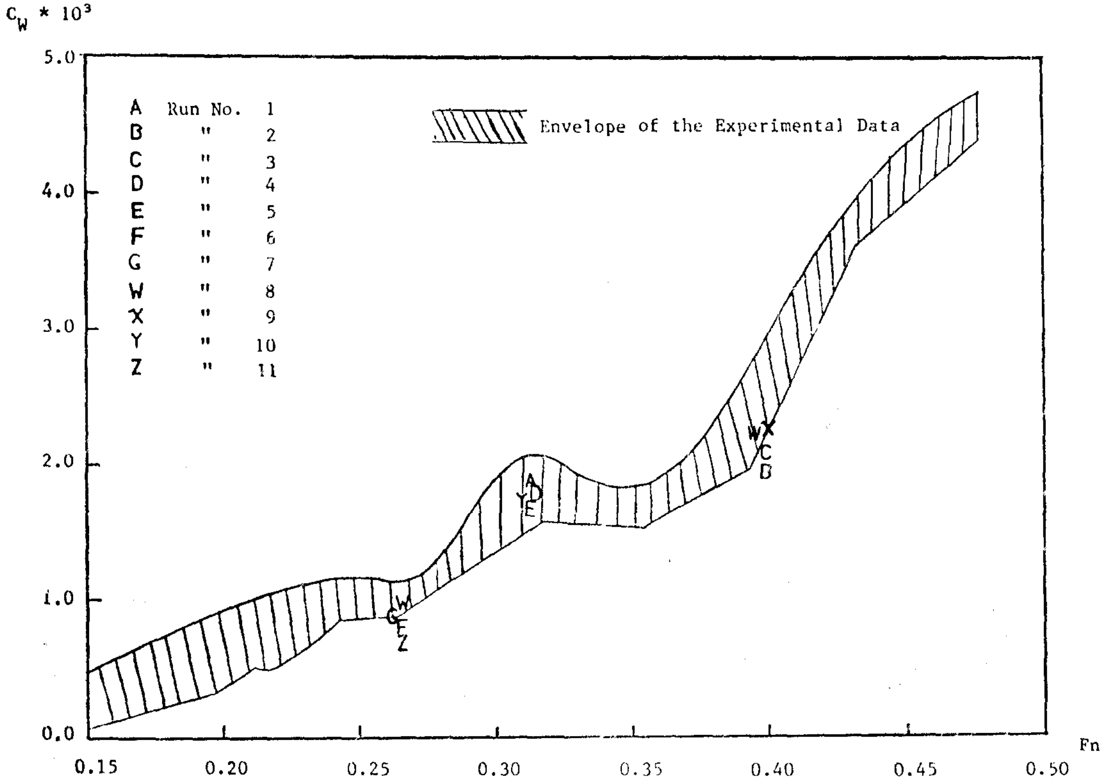

Fig. 2 Comparisos of wavemaking resistance coefficients calculated for 11 test cases

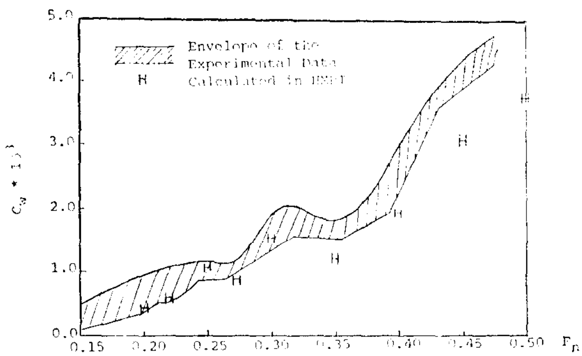

Fig. 3 Comparisons of wavemaking resistances calculated by the program of HMRI and measured

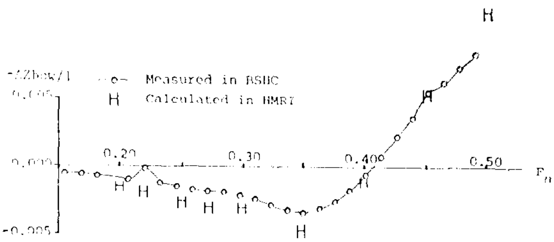

Fig. 4 Comparisons of sinkage at the bow measured and calculated

than run No. 7, and by about 14% at the value of Froude No. being 0.402 than run No. 2, wheras it is decreased a little at 0.313 of Froude No. than run No. 2.

The calculated results for the different panel arrangements on the hull surface show no systematic changes, but slight differences each other. However, the wave resistance is generally increased by the enlargement of the free surface region and No. of strips in the y-direction, with considerable difference. In comparison with measured results as shown in Fig. 2, it is thought that a larger free surface portion is required for high Froude numbers, while smaller panels are needed for low Froude numbers.

Therefore, for the comparative calculations for different ships, it is considered to be better that the calculation is done under the same condition of the panel arrangement and the free surface region, which is to be determined in the basis of design speed, etc.

For the further calculation, run No. 10 was chosen. The wavemaking resistances calculated by the panel arrangement condition of run No. 10 were compared with the measured results[12] as shown in Fig. 3.

The calculated results show a good agreement of tendancy with the measured values, but, there is a large difference for the Froude No. larger than 0.3. And the calculated values of sinkage at the bow were compared with the measured values [8] in Bulgarian Ship Hydrodynamic Centre (BSHC) as shown in Fig. 4. The calculated values of HMRI follow the measured curve quite well.

The comparisons between the calculated wave

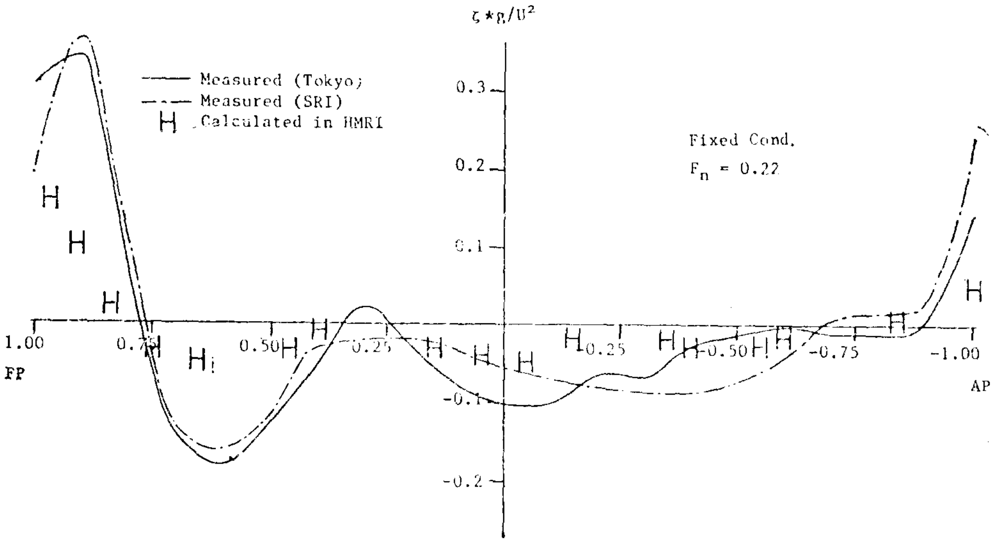

Fig. 5 Comparisons of wave profiles for Wigley hull calculated and measured at Fn=0.22

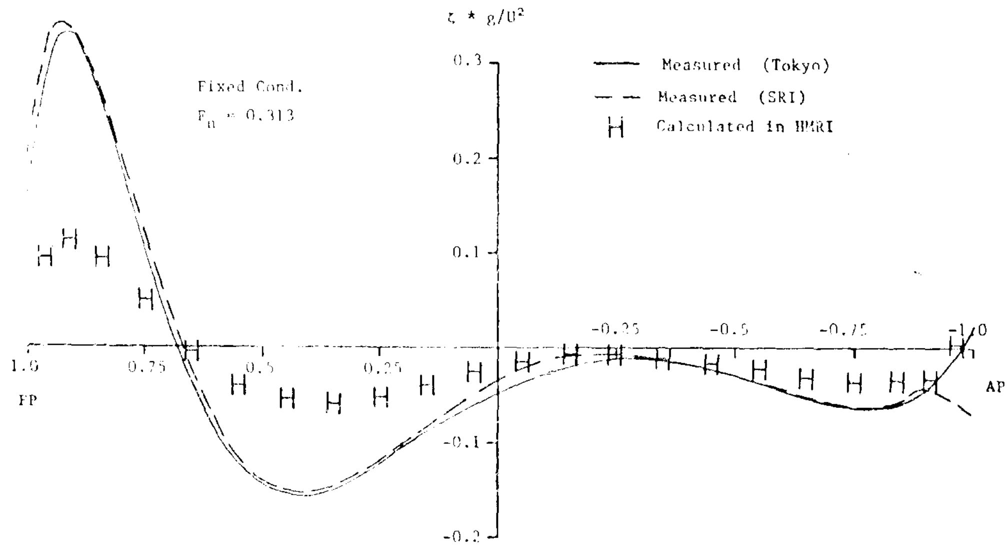

Fig. 6 Comparisons of wave profiles for Wigley hull calculated and measured at Fn=0.313

profiles and measurements were made for 0.22, 0.313 of Froude No., which are shown in Fig. 5 and 6. In case of 0.22 of Froude No., there is a large discrepancy between the two sets of values and a phase seems to shift. In case of 0.313 of Froude No., the phase is almost the same but there is a fairly large difference in the magnitude at the first crest and hollow.

The calculated values of pressure distribution on the hull surface at 0.25, 0.313 of Froude No. were compared with the measurement values of IHI [13] as shown in Fig. 7 and 8. The results of present

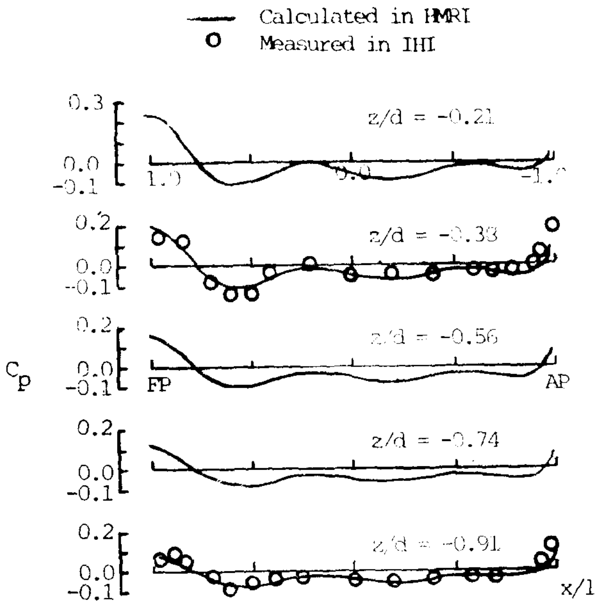

Fig. 7 Pressure distribution on the surface of Wigley Hull at Fn=0.250

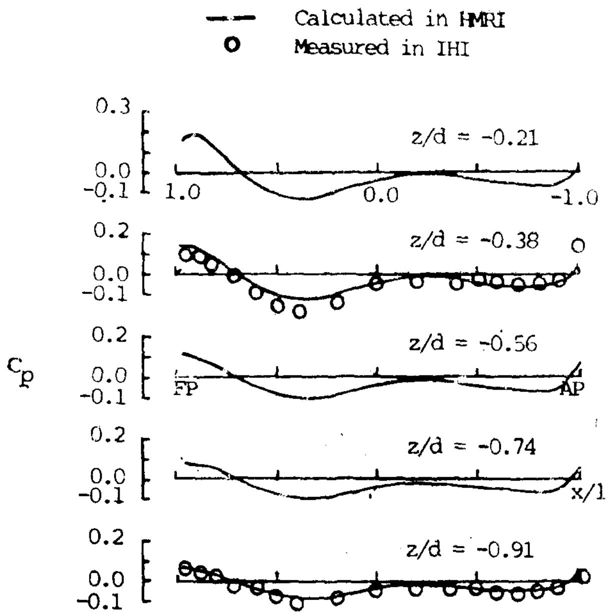

Fig. 8 Pressure distribution on the surface of Wigley hull at Fn=0.313

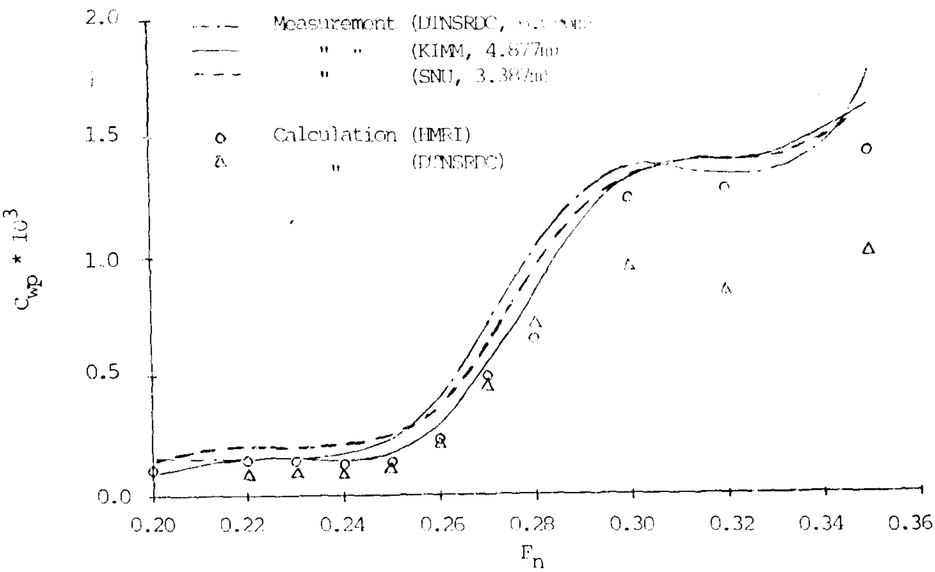

Fig. 9 Comparisons of wavemaking resistances for series 60 hull in the fixed condition

calculation show the good agreement with the measured values.

4.2. Series 60, $C_b=0.60$

6 rows of panels from the keel to the undisturbed free surface and 24 divisions from FP to AP represent the Series 60 ship with $C_b=0.60$ and the local region of the free surface with $-2.0\leq x/l\leq 1.5$, $0\leq y/l\leq 0.775$ was represented by 38×10 panels.

The wavemaking resistances were calculated at Fn=0.20~0.35 and were compared with the measured and the calculated values in DTNSRDC [14] as shown in Fig. 9. The calculated results follow the experimental curves very well, but the big differences in the calculated values in HMRI & DTNSRDC appear at more than Fn=0.30. Its discrepancy is probaby due to the different panel arrangements on the hull surface and the free surface, which is 26×8 panels for the hull surface and 36×8 panels for the free surface with the region of $-1.5\leq x/l\leq 1.5$, $0\leq y/l\leq 0.7$.

The wave profiles were calculated at the range of Fn=0.20~0.35 and were compared with the measured values in DTNSRDC[14] as shown in Fig. 10. The calcualted wave profiles show the good agreement of tendancy with the measured values at each Froude Noumber, but the prediction always underestimates the magnitude of the first crest and overestimates the one of the last crest.

In Fig. 11, 12 and 13, the calcualted wave profiles were compared with the measured values in HMRI, KIMM and SNU[15]. In case of Fn=0.22, it is seen that the tendancy is almost same, but the phase

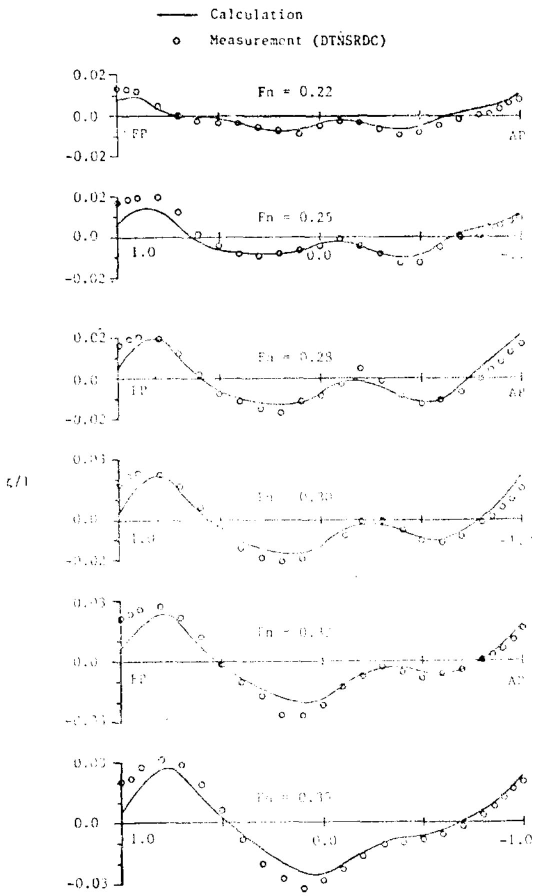

Fig. 10. Comparisons of wave profiles for series 60 hull in the fixed condition

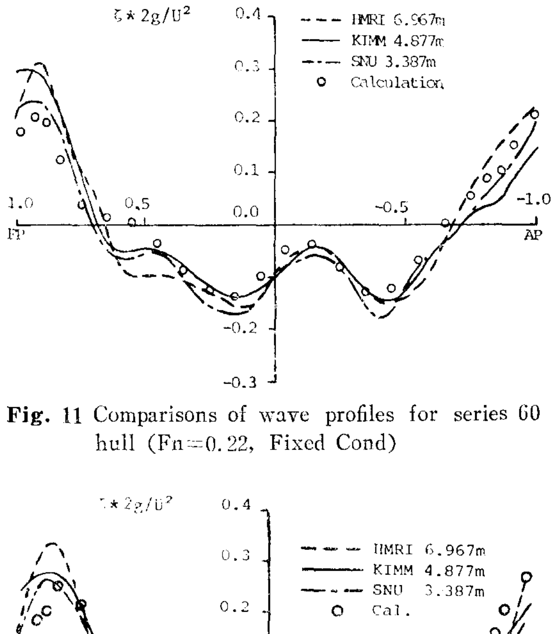

Fig. 11 Comparisons of wave profiles for series 60 hull (Fn=0.22, Fixed Cond)

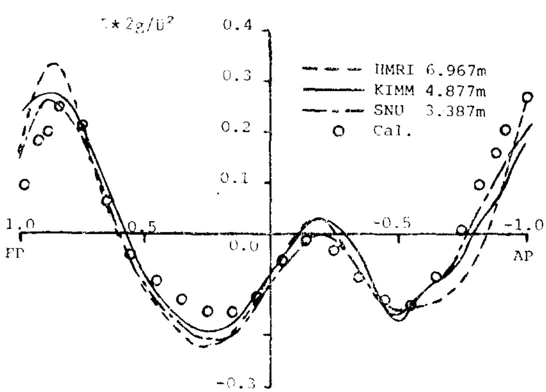

Fig. 12 Comparisons of wave profiles for series 60 hull (Fn=0.28, Fixed Cond)

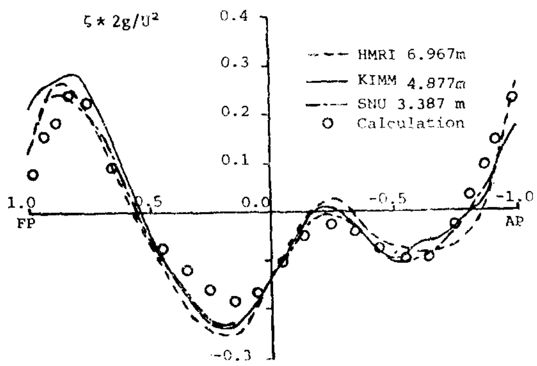

Fig. 13 Comparisons of wave profiles for series 60 hull (Fn=0.30, Fixed Cond)

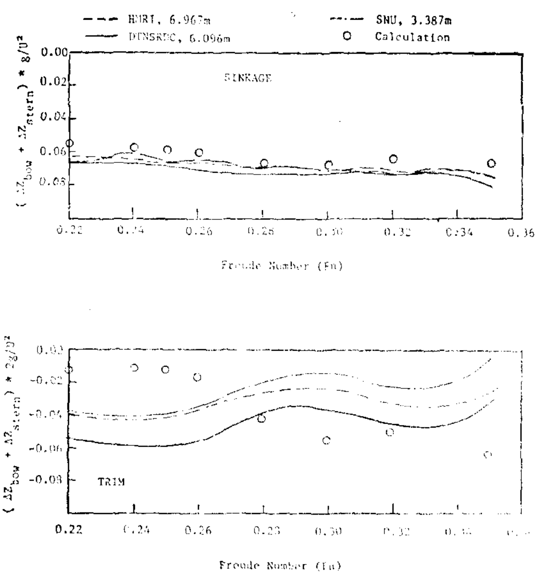

Fig. 14 Comparisons of sinkage and trim for series 60 hull

seems to shift as shown in Fig. 11. For Fn=0.28, 0.30, the maginitude of the first & end crest and the first hollow has been underestimated, but the calculated values follow the experimental curves very well as shown in Fig. 12 and 13. The fact that the predeicted stern wave is too large is most probably due to the neglect of viscosity, i.e. the boundary layer displacement effect.

In Fig. 14 are shown comparisons of the calculated and the measured sinkage and trim. There are considerable differences between three sets of the measured values for trim.

The agreement of tendancy seems fairly good for the sinkage curve, but the trim curve displays discrepancy, expecially at low Froude Noumbers.

5. Conclusions

Following remarks can be mentioned as conclusions of the present report.

1) The present method based on the method using the Rankine source distribution over the hull surface and undisturbed free surface was applied to evaluate the flow field, wave pattern and wave resistance.

2) The calculated values of wave resistance, trim & sinkage and pressure distribution agree with the measured values quite well, except the range of high Froude numbers.

3) The calculated results depend to a certain extent on the discretization of the hull surface and especially of the free surface. Similar panel arrangements should therefore be used in case of the comparative calculations for different competing ship forms, etc.

4) Smaller panels should be used for low Froude numbers, while a larger free surface portion is required for high Froude numbers.

References

[1] Hess, J.L. & Smith, A.M.O., "Calculation of Non-Lifting Potential Flow about Arbitrary Three-Dimensional Bodies", Douglas Report No. ES 40622(1962).

[2] Gadd, G.E., "A Method of Computing the Flow and Surface Wave Pattern Around Full Forms", The Royal Institution of Naval Architects, Volume 118(1976).

[3] Dawson, C.W., "A Practical Computer Method for Solving Ship-Wave Ploblems", 2nd International Conference on Numerical Ship Hydrodynamics (1977).

[4] Mori, K., "Prediction of Flow Fields Around Ship by Modified Rankine Source Method (1st Report)", *Journal of Soc. Nav. Arch. Japan,*

Vol. 150 (1981).

[5] Ogiwara S., "A Method to Predict Free Surface Flow Around Ship by Means of Rankine Sources", *Journal of Kansai Soc. of Nav. Arch. Japan*, No. 190 (1983).

[6] Dawson, C.W., "Calculations with the XYZ Free Surface Program for Five Ship Models", *Proceedings of Workshop on Ship Wave-Resistance Computations*, DTNSRDC (1979).

[7] Xia Fei, "Calculation of Potential Flow with a Free Surface", the Report of Chalmers University of Technology, Report No. 65 (1984).

[8] D.K. Lee, "The Use of Rankine Source to Evaluate Velocities Around a Ship Hull", *SNAK*, Vol. 18, No. 4 (1981).

[9] S.H. Van, "Numerical Calculations of the Flow Around a Ship by Rankine Source Distributions", Report No. UDC 629.112, the Ministry of Science & Technology (1988).

[10] Lee, C.S., Yang, S.I., Kang, C.G., "A Note on the Rankine Source Method for Free Surface Flow Problem; Radiation Condition & Influence of Truncation of Source Distribution", *Proc. of 16th ITTC* (1981).

[11] Joa, S.W., "A Study on the Calculation of Wavemaking Resistance by the Singularity on a Ship Surface(1st Report)", *Hyundai Technical Review*, Vol. 3, No. 4 (1983).

[12] Report of the 17th ITTC Resistance Committee (1984).

[13] The Report of Cooperative Experiments on Wigley Parabolic Models in Japan, Presneted to the Resistance Committee of the 17th ITTC, Varna (Sept. 1983).

[14] Kim, Y.H. & Jenkins, D., "Trim & Sinkage Effects on Wave Resistance with Series 60, $C_B=0.60$", DTNSRDC/SPD-1013-01 (1981)

[15] Kim, H.C. et al., "Report on the Cooperative Experimental Study Program", *SNAK*, Vol. 24, No. 3 (1987).